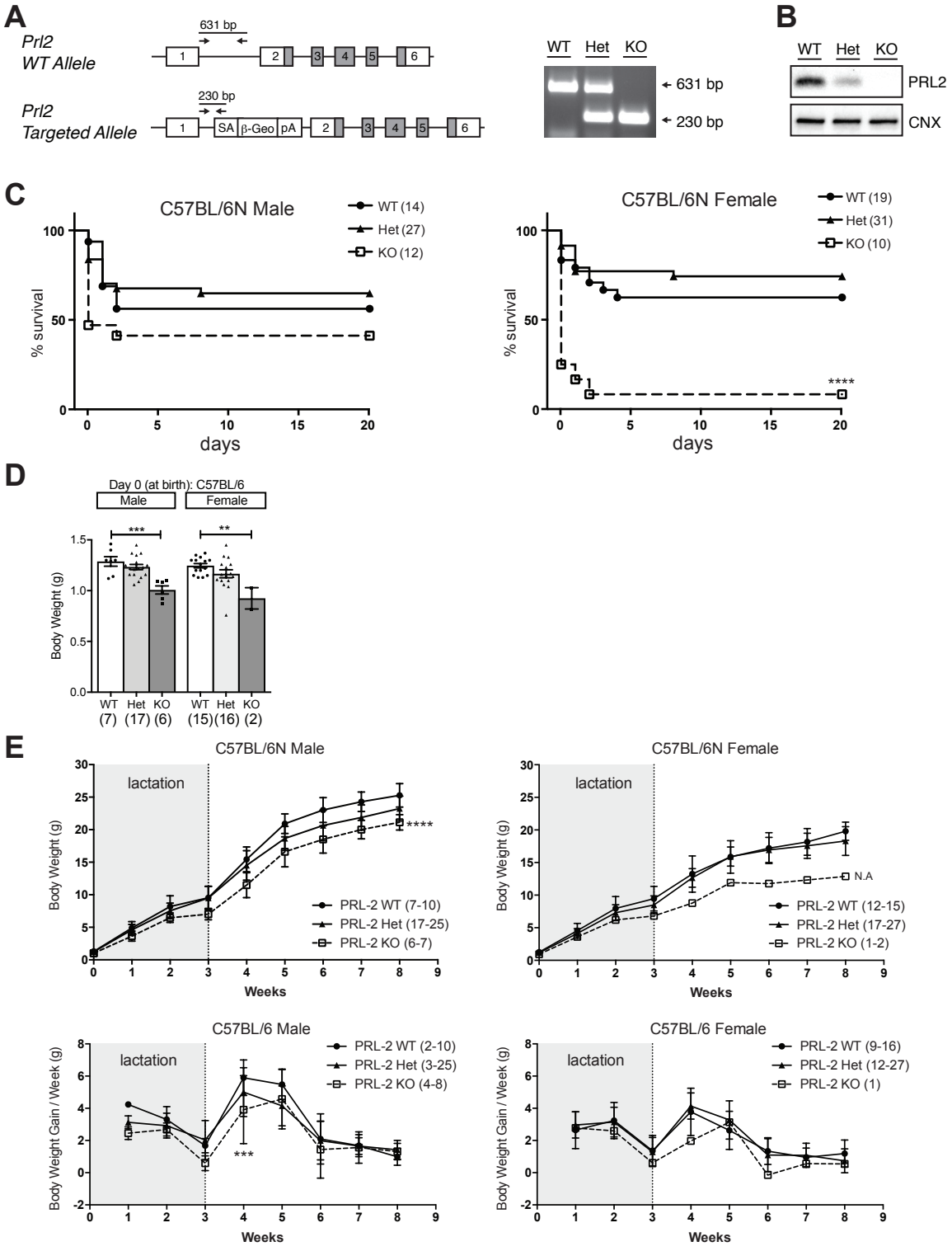

Supplemental figure S1

Gender-dependent differences in viability of the PRL2 KO mice in C57BL/6N background

(A) Generation of the PRL2 (PTP4A2) deficient mice. Schematic genomic construction of the targeted allele for *Prl2* (*Ptp4a2*) gene is shown. The trapping vector was inserted between exon 1 and exon 2 of the gene coding for PRL2. Arrows indicate PCR primers used for genotyping. (A, right) PCR genotyping was performed on genomic DNA. Predicted sizes of PCR products were obtained for WT, heterozygous and mutant alleles. (B) Protein was extracted from skeletal muscle and immunoblotted with PRL1/2 and calnexin (CNX) antibodies. (C) % survival of the mice after birth was plotted for both male (left) and female (right). ****p<0.0001 (WT vs KO), Log-rank (Gehan-Breslow-Wilcoxon) test. (D) Average body weight at birth for each genotype are shown. (E) Average body weight for each genotype (top) and body weight gain per week (bottom) were plotted every week from birth to 8 weeks. *P* values were calculated by one-way ANOVA with Dunnet's multiple comparison test (D), two-way ANOVA with Dunnett's multiple comparison test (E), **p*<0.05, ***p*<0.01, ****p*<0.001, *****p*<0.0001

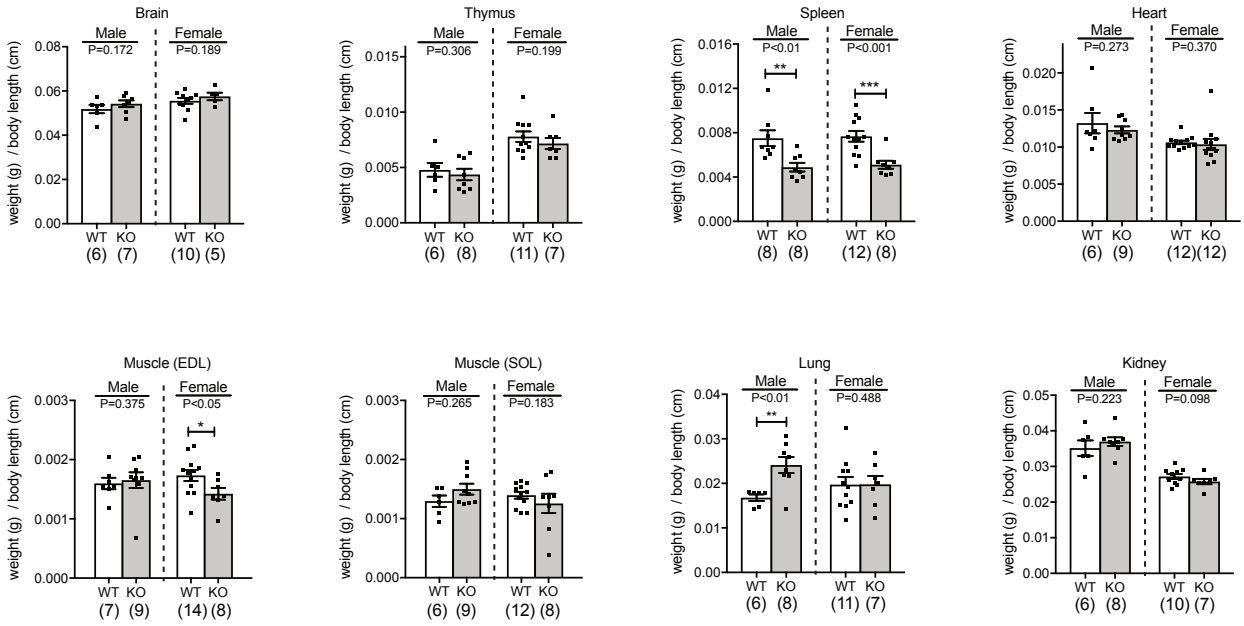

Supplemental figure S2
Body composition of PRL2 KO mice
Dissected tissue weights were normalized by body length and mean values were plotted. Data is expressed as mean ± SEM. Statistical analysis was performed by Student's *t*-test (**p*<0.05, ***p*<0.01, ****p*<0.001). EDL: extensor digitorum longus muscle, SOL: soleus muscle.

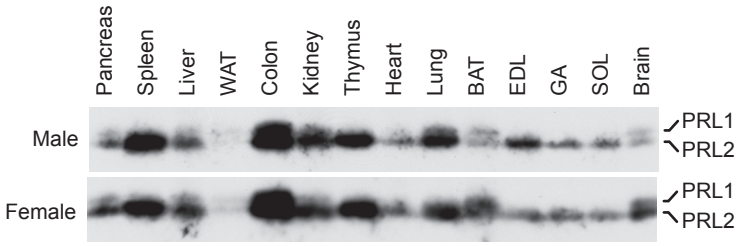

Supplemental figure S3
PRL1/2 protein expression pattern in major tissues
Tissue distribution of PRL1 and PRL2 proteins is shown. Tissues were lysed, then male and female tissues were separately loaded on the gels and immunoblotted with PRL1/2. EDL: extensor digitorum longus muscle, GA: gastrocnemius muscle, SOL: soleus muscle.

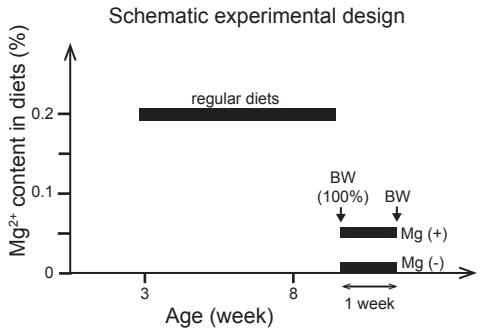

Supplemental figure S4
Schematic experimental design for dietary Mg^{2+} depletion

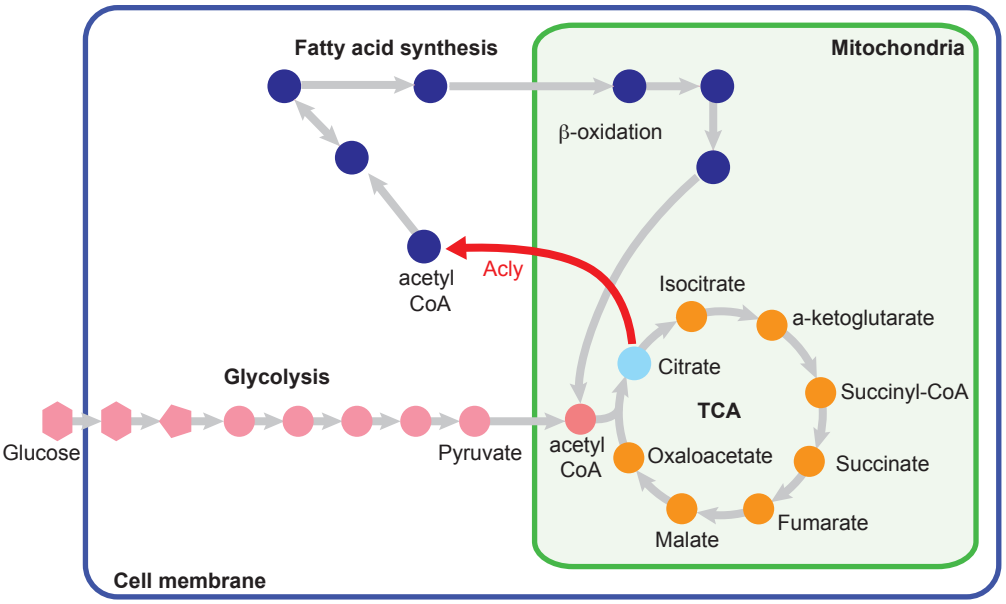

Supplemental figure S5
Schematic overview of the metabolic pathway
Major cellular metabolic pathways are schematically drawn. The process where Acly act are indicated by a red arrow.

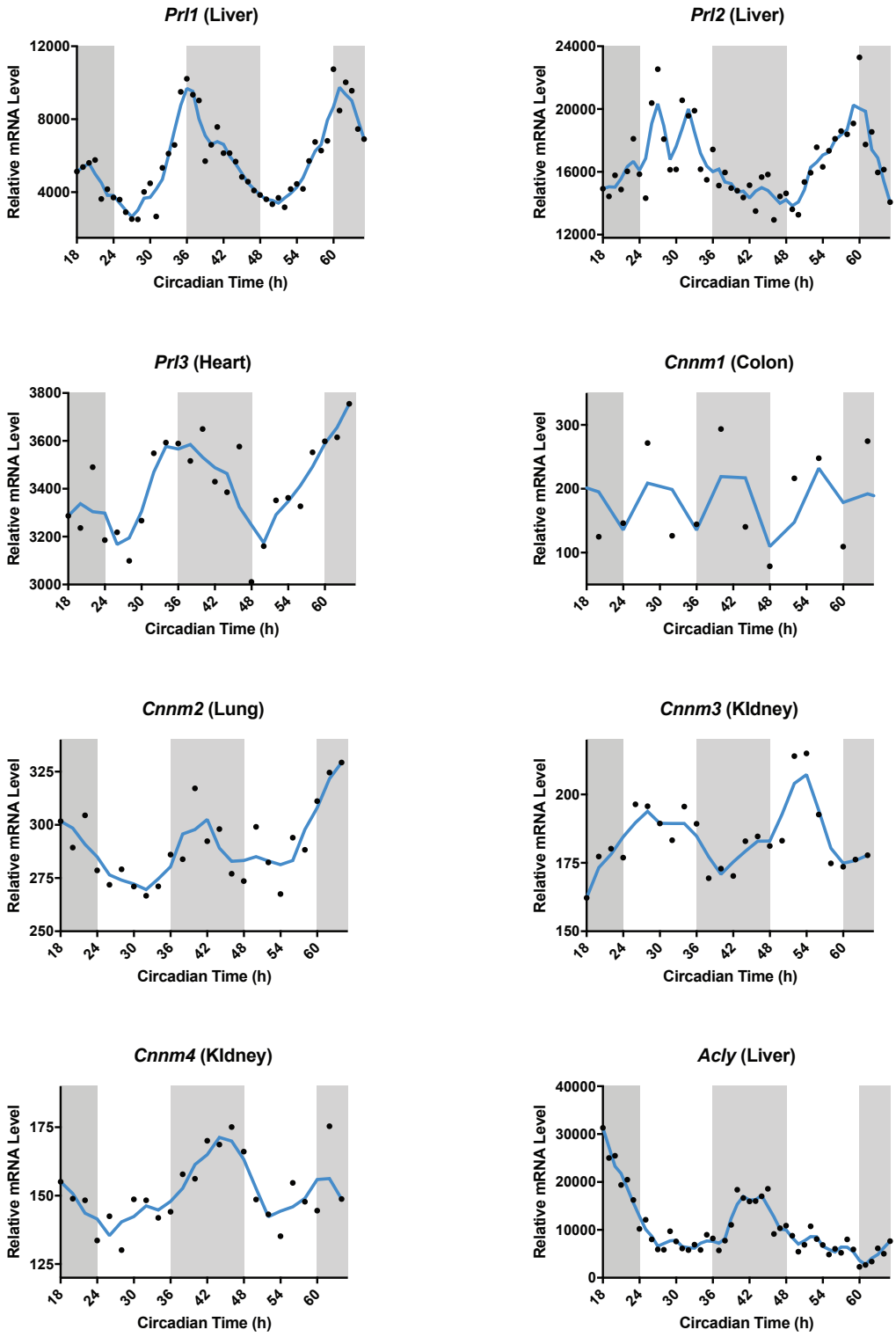

Supplemental figure S6
Relative mRNA levels of *Prl* and *Cnnm* family genes from publically available micro-array data[1-3]

1. Hughes, M.E., et al., Harmonics of circadian gene transcription in mammals. PLoS Genet, 2009. 5(4): p. e1000442.
2. Zhang, R., et al., A circadian gene expression atlas in mammals: implications for biology and medicine. Proc Natl Acad Sci U S A, 2014. 111(45): p. 16219-24.
3. Hoogerwerf, W.A., et al., Transcriptional profiling of mRNA expression in the mouse distal colon. Gastroenterology, 2008. 135(6): p. 2019-29.

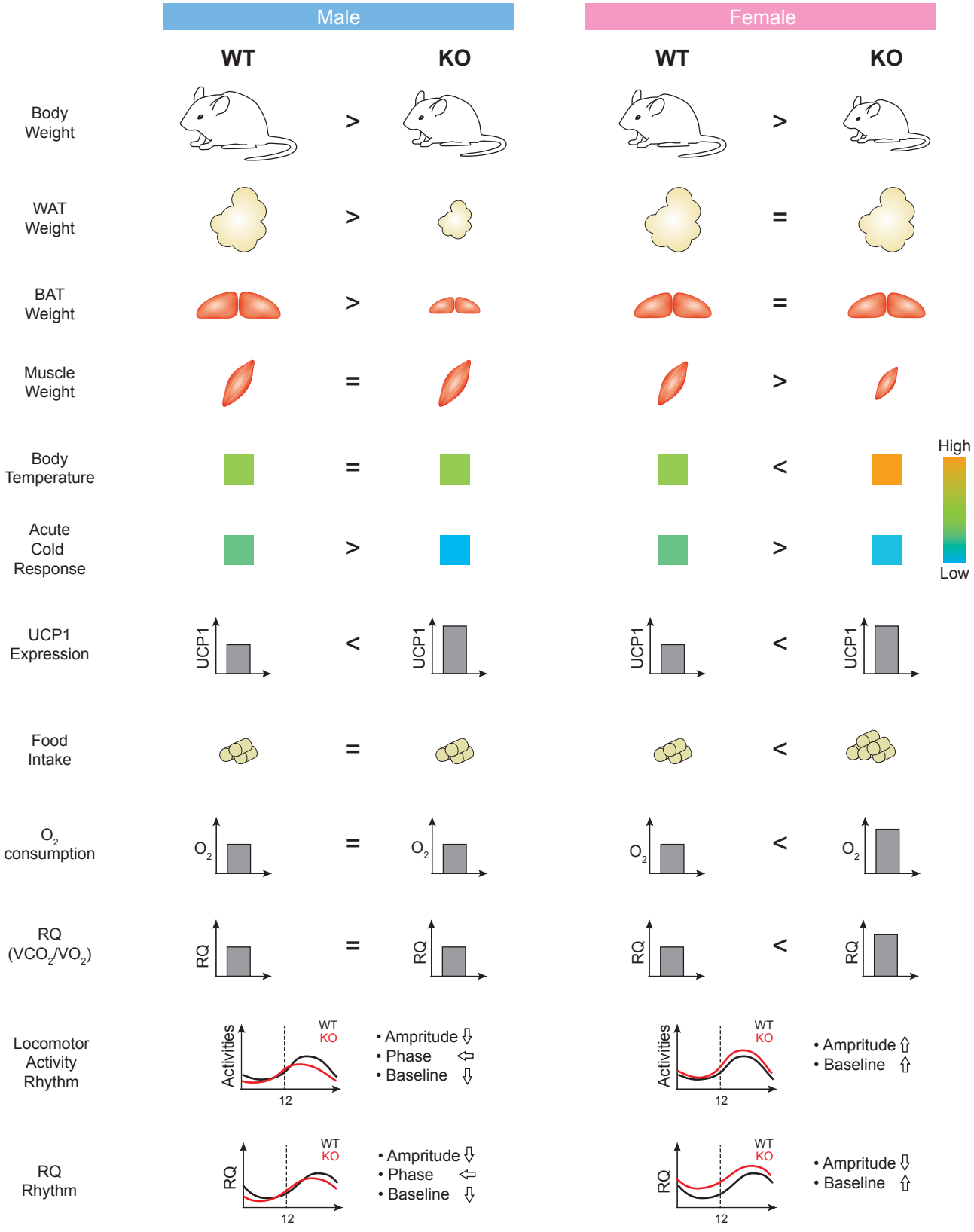

Supplemental figure S7
Graphical summary of PRL2 KO mice phenotypes

Supplemental experimental procedure

Quantitative real-time PCR

Primers used for Figure 3D

Target gene (mouse)	Primer sequence (5' to 3')
β-Actin, forward	GGACTCCTATGTGGGTGACG
β-Actin, reverse	GGGAGAGCATAGCCCTCGTA
PRL-3, forward	AAGGACGGCATCACTGTTGT
PRL-3, reverse	GCTTCCCGGGTCATTGTAGA

Primers used for Figure 6H

Target gene (mouse)	Primer sequence (5' to 3')
Tbp, forward	ACCTTATGCTCAGGGCTTGG
Tbp, reverse	GCCATAAGGCATCATTGGAC
Cs, forward	ATCCATAGTGACCATGAGGG
Cs, reverse	TCAGTGCCTCAGATACAGTTT
Fh1, forward	TTGGACAGGAATTCAGTGGT
Fh1, reverse	ATCGCTTCACACTGAGTAGG
Acc, forward	GTCCCCAGGGATGAACCAATA
Acc, reverse	GCCATGCTCAACCAAAGTAGC
Fasn, forward	GGAGGTGGTGATAGCCGGTAT
Fasn, reverse	TGGGTAATCCATAGAGCCCAG
Acly, forward	AAGCCTTTGACAGCGGCATCATTC
Acly, reverse	TTGAGGATCTGCACTCGCATGTCT
Cox7a1, forward	CAGTACACTTGAAAGGCGGG
Cox7a1, reverse	CCAGCCCAAGCAGTATAAGC
Atp5j, forward	GGCCGGAAGTAGAACGGT
Atp5j, reverse	GAGACTGCTGACCGAAGGAC